

Measurements of Hydrate Dissociation Temperature of Gas Mixtures in the Absence of Any Aqueous Phase and Prediction with the Cubic-Plus-Association Equation of State

Ziad Youssef,[†] Alain Barreau,[†] Pascal Mougín,^{*,†} Jacques Jose,[‡] and Ilham Mokbel[‡]

IFP, 1-4 avenue de Bois Préau 92852 Reuil-Malmaison Cedex, France, and UMR 5180, Université Claude Bernard Lyon I, 43 bvd du 11 Novembre 1918, 69622 Villeurbanne Cedex, France

Gas hydrate formation is undesired in processing and gas distribution. Therefore, it is important to have a thermodynamic model that predicts correctly gas hydrate formation. Hydrate formation is very well studied in the literature in the presence of liquid water, and hydrate thermodynamic models predict correctly its formation; however, there is little information about gas hydrate formation without an aqueous phase. The new experimental procedure combining an equilibrium cell with water measurement by a Karl Fischer coulometer developed in our previous work (Youssef et al. *Ind. Eng. Chem. Res.* **2009**, *48*, 4045–4050) was used to determine the hydrate dissociation temperature in the absence of an aqueous phase on three gas mixtures at different pressures and for different amounts of water content. As in previous work, the classical Platteeuw and van der Waals model associated to the cubic plus association (CPA) equation of state, used in a totally predictive way, correctly predict hydrate dissociation with or without an aqueous phase for the gas mixtures.

Introduction

In the twentieth century, with the expansion of the natural gas industry, operations involving gases were operated at high pressure. It was discovered that pipelines were plugged with components similar to ice, whereas the conditions were too warm for ice to be formed. Later on, Hammerschmidt¹ demonstrated that what was formed is not ice, but gas hydrates.

In general, hydrates are formed at high pressures and low temperatures. Water molecules form a lattice structure, and the gas molecules occupy the interstitial vacancies of the lattice. The phenomena of inclusion of the guest molecule and the van der Waals attraction between water and gases stabilize the hydrate crystal structure. It is generally assumed that the gas molecules can vibrate and rotate freely within these vacancies or cavities. Another assumption is that the gas molecules are too large to move freely through the lattice and each one is localized in a single cavity.

The gas hydrate crystalline structure is mainly one of the following: cubic structure I (sI), cubic structure II (sII), or hexagonal structure H (sH) (Sloan²). In the past, the presence of liquid water was supposed necessary for gas hydrate formation. Nowadays it has been shown that hydrates could be formed in the absence of liquid water. A strong argument demonstrating that liquid water is not necessary for hydrate formation was given by Carroll:³ the frost can sublime from air (vapor) to ice (solid) on winter nights.

In the industrial applications and gas transportation, the hydrate formation is undesired and risky even in the absence of an aqueous phase. To correctly design a dehydration unit,

it is very important to determine the conditions in which the hydrate will be formed. These conditions are functions of the thermodynamics and kinetics.

Hydrate formation has been very well studied in the literature in the presence of an aqueous phase, but few studies in the literature describe a hydrate formation in the absence of liquid water. As examples, Aoyagi et al.⁴ and Song et al.⁵ have measured vapor-hydrate equilibrium with methane, and Song and Kobayashi^{6,7} have reported vapor-hydrate equilibrium with ethane and CO₂. The hydrate dissociation temperature measurements on gas mixtures without an aqueous phase are scarce. Song and Kobayashi⁸ measured the hydrate dissociation temperatures of the CH₄ (1) + C₃H₈ (2) gas mixture with $x(\text{CH}_4) = 0.9469$ and $x(\text{H}_2\text{O})$ from $1.15 \cdot 10^{-6}$ up to $427 \cdot 10^{-6}$ and for pressures from (2.07 to 10.34) MPa. Aoyagi and Kobayashi⁹ have measured the hydrate dissociation temperatures of the CH₄ (1) + C₂H₆ (2) + C₃H₈ (3) + CO₂ (4) gas mixture ($x(\text{CH}_4) = 0.7502$, $x(\text{C}_2\text{H}_6) = 0.0795$, $x(\text{C}_3\text{H}_8) = 0.0399$, $x(\text{CO}_2) = 0.1304$) with $x(\text{H}_2\text{O})$ from $2.50 \cdot 10^{-6}$ up to $99 \cdot 10^{-6}$ and for pressures from (45.8 to 120.9) MPa. More recently, Chapoy et al.¹⁰ have studied two gas mixtures in such conditions. The first one is composed by CH₄ (1) + C₂H₆ (2) + C₃H₈ (3) + $n\text{C}_4\text{H}_{10}$ (4), and measurements have been performed from (250 to 290) K with an amount of water in the range of $8 \cdot 10^{-6}$ to $265 \cdot 10^{-6}$ mole fraction. The second gas is composed by CH₄ (1) + C₂H₆ (2) + C₃H₈ (3) + N₂ (4) + CO₂ (5), and it has been studied in the same range of conditions.

Hydrates thermodynamic models based on van der Waals and Platteeuw¹¹ theory are generally based on data in the presence of an aqueous phase, and they predict correctly its formation when an aqueous phase is formed. As there are limited hydrate data without the aqueous phase, this situation is more difficult to predict.

* To whom correspondence should be addressed. Tel.: +33 1 47 52 66 25. Fax: +33 1 47 52 70 25. E-mail: pascal.mougin@ifp.fr.

[†] IFP.

[‡] UMR 5180, Université Claude Bernard Lyon I.

Table 1. Mole Fractions of the Gas Mixtures

	$x(\text{CH}_4)$	$x(\text{C}_2\text{H}_6)$	$x(\text{C}_3\text{H}_8)$	$x(\text{CO}_2)$
gas mixture 1	0.9468		0.0532	
gas mixture 2	0.5996	0.1001		0.3003
gas mixture 3	0.82995	0.0800	0.03005	0.0600

In a previous work,¹² we presented a new experimental procedure to determine the hydrate dissociation temperature in the absence of any aqueous phase. The dissociation temperatures for methane hydrate, ethane hydrate, and carbon dioxide hydrate were determined at different pressures and for different water amounts. In other hand, we have been shown that the classical Platteeuw and van der Waals model associated with the cubic plus association (CPA) equation of state is able to predict well the hydrate dissociation temperature without an aqueous phase.

After having studied hydrate formation in the presence of a single gas, in the present work, new experimental results of the hydrate dissociation temperature for different gas mixtures without an aqueous phase are presented. These new data are also modeled with the same approach.

Experimental Study

The experimental method to detect the hydrate dissociation temperature has been presented in a previous work.¹² It consists of measuring the water content in the vapor phase as a function of the equilibrium cell temperature. Prior to hydrate formation, the water content in the vapor phase is constant with temperature. When the quantity of water in the vapor phase drops, it is assumed that the water was consumed to form hydrate. The hydrate dissociation temperature is then the intersection point due to the slope change of the curve representing the amount of water in the vapor phase versus temperature. This intersection should be obtained graphically. Taking into account the uncertainty of the water contents of the vapor phase, various fitting curves have been obtained, and they are used to estimate the

uncertainty on the determined temperature of dissociation. This uncertainty has been estimated to be about ± 0.5 K.

Materials. The gas mixtures were prepared by Air Liquide. The desired water amounts are obtained by injecting a few microliters of liquid water at ambient temperature into the equilibrium cell. The gas mixture is then introduced at the desired pressure, and agitation is set up to obtain an homogeneous vapor phase. Table 1 gives the composition for each mixture. The uncertainty of the dry mole composition of the mixtures is about 0.1 %.

Experimental Apparatus and Procedure. The experimental apparatus and procedure are described in detail by Youssef et al.¹² The equilibrium cell is filled with the mixture at room temperature and at a fixed pressure. The pressure sensor of the equilibrium cell has been calibrated with an accuracy within 0.001 MPa, and the uncertainty of the temperature probe is about 0.05 K.

The water content of the fluid in the monophasic region is then determined at different temperatures. Thereafter, the temperature is decreased to its lowest possible value to obtain hydrates. Then, the water content of the vapor phase is determined as a function of the temperature of the equilibrium cell. A Karl Fischer coulometer was used to measure the very small amount of water in the vapor phase. Its accuracy on the measured water content is about ± 5.0 %.

The temperature rate of the cell during the decrease and increase is very low to avoid the formation of ice or metastable water. Once the water content of the mixture is in the vapor domain, we carry on the first measurement in the presence of hydrate at the lower temperature. In this case, the driving force which induces the hydrate formation is the most important, and no free water should remain for ice formation. In addition, the studied pressures are defined in order not to form liquid hydrocarbon phase under the experimental temperature domain.

Every single experimental data point represents the average of at least three measurements at the same temperature. The interval between two measurements is more than 3 h, and the

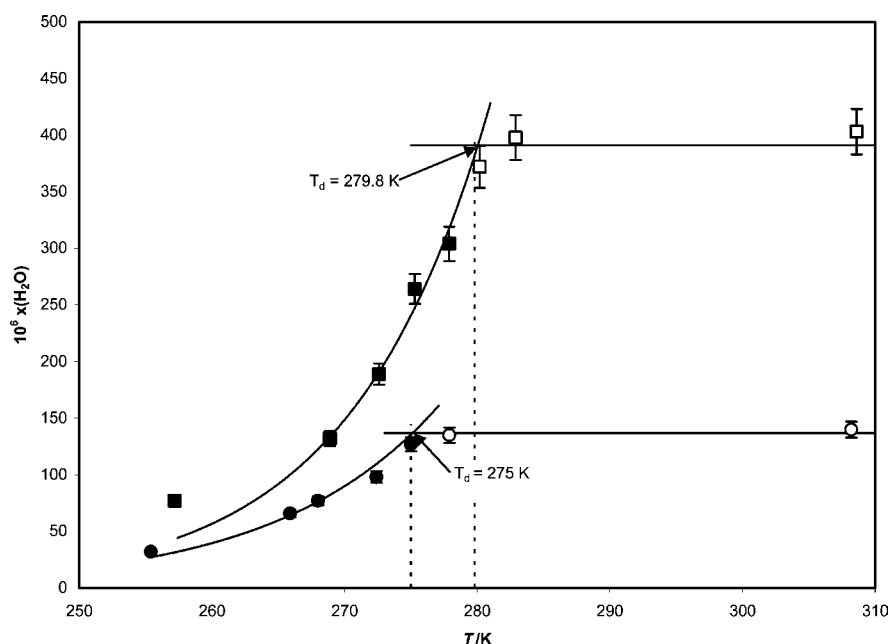


Figure 1. Water content of the vapor phase as a function of temperature for the gas mixture 1: $\text{CH}_4 + \text{C}_3\text{H}_8$. \circ , \bullet , pressure = 5.0 MPa and $x(\text{H}_2\text{O}) = 137 \cdot 10^{-6}$ in the vapor and vapor-hydrate domain. \blacksquare , \square , pressure = 2.07 MPa and $x(\text{H}_2\text{O}) = 391 \cdot 10^{-6}$ in the vapor and vapor-hydrate domain.

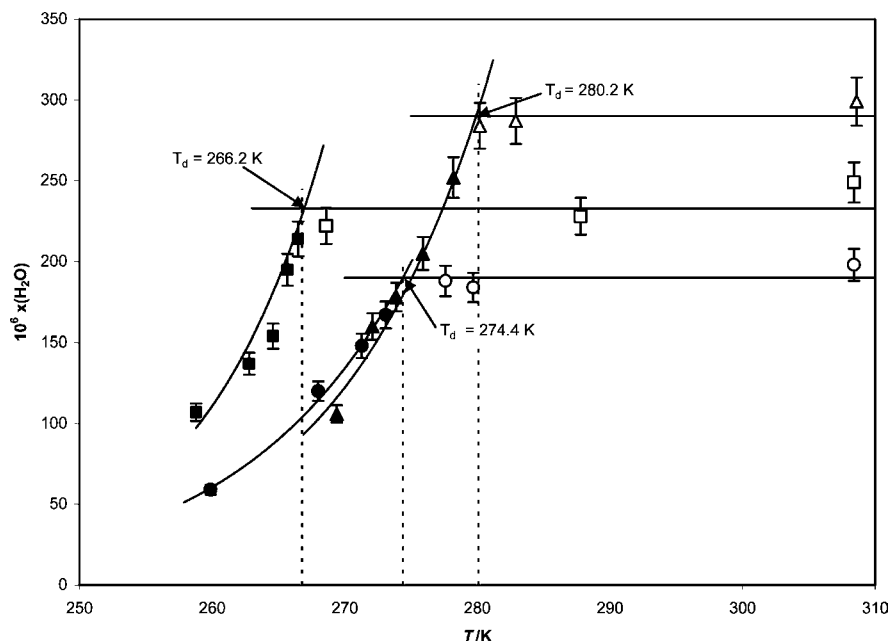


Figure 2. Water content of the vapor phase as a function of temperature for the gas mixture 2: $\text{CH}_4 + \text{C}_2\text{H}_6 + \text{CO}_2$. \circ , \bullet , pressure = 4.0 MPa and $x(\text{H}_2\text{O}) = 190 \cdot 10^{-6}$ in the vapor and vapor-hydrate domain. \blacktriangle , \triangle , pressure = 4.0 MPa and $x(\text{H}_2\text{O}) = 290 \cdot 10^{-6}$ in the vapor and vapor-hydrate domain. \blacksquare , \square , pressure = 1.33 MPa and $x(\text{H}_2\text{O}) = 233 \cdot 10^{-6}$ in the vapor and vapor-hydrate domain.

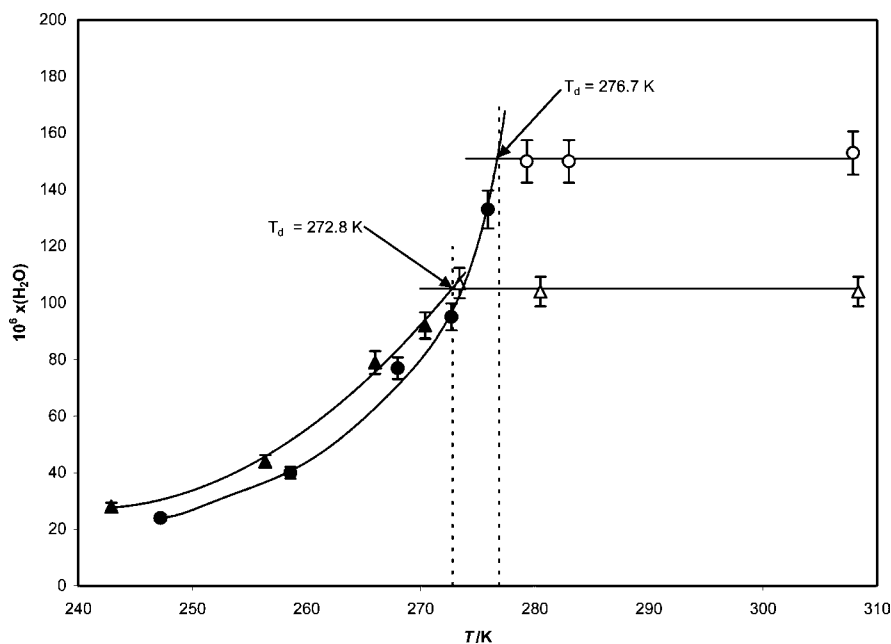


Figure 3. Water content of the vapor phase as a function of temperature for the gas mixture 3: $\text{CH}_4 + \text{C}_2\text{H}_6 + \text{C}_3\text{H}_8 + \text{CO}_2$. \circ , \bullet , pressure = 5.06 MPa and $x(\text{H}_2\text{O}) = 151 \cdot 10^{-6}$ in the vapor and vapor-hydrate domain. \blacktriangle , \triangle , pressure = 7.0 MPa and $x(\text{H}_2\text{O}) = 105 \cdot 10^{-6}$ in the vapor and vapor-hydrate domain.

relative deviation of the water content is less than 10 %. Each experimental series took around (2 to 3) weeks to be accomplished.

Experimental Results. Hydrate dissociation temperature measurements were performed by studying three different gas mixtures composed of $\text{CH}_4 + \text{C}_3\text{H}_8$ for the gas mixture 1, $\text{CH}_4 + \text{C}_2\text{H}_6 + \text{CO}_2$ for the gas mixture 2, and $\text{CH}_4 + \text{C}_2\text{H}_6 + \text{C}_3\text{H}_8 + \text{CO}_2$ for the gas mixture 3 at different pressures and for different water amounts. The mole fractions of the components of the mixtures are reported in Table 1. Under our experimental conditions, no liquid water phase was formed. The curves on Figures 1, 2, and 3 are calculated from the experimental points and are given the temperature of dissociation of the hydrates. Each point has been indicated with its error bar which is the

uncertainty of the water content in the vapor phase measured with the Karl Fischer coulometer. As mentioned early, this uncertainty is around 5 %. The determination of such lower water contents of the vapor phase is difficult, and they should be perturbed for example by adsorption in tubes or by small fluctuations of the temperature or the pressure in the sample line. Figures 1, 2, and 3 show the advantage of the proposed method, which is fitting various water contents along the temperature profile.

The gas mixture 1 was studied at (5.0 and 2.07) MPa with respectively $x(\text{H}_2\text{O})$ between $(137 \pm 7) \cdot 10^{-6}$ and $(391 \pm 20) \cdot 10^{-6}$. The water content in the vapor phase versus temperature curves are shown in Figure 1. The hydrate dissociation temperatures were respectively (275.0 and 279.8) K. The latter

Table 2. Summary of the Experimental Hydrate Dissociation Temperatures

$10^6 x(\text{H}_2\text{O})$	P/MPa	T/K
Gas Mixture 1: $\text{CH}_4 + \text{C}_3\text{H}_8$		
137	5.0	275.0
391	2.07	279.8
427 ⁸	2.07	277.2
Gas Mixture 2: $\text{CH}_4 + \text{C}_2\text{H}_6 + \text{CO}_2$		
190	4.0	274.4
290	4.0	280.2
233	1.3	266.2
Gas Mixture 3: $\text{CH}_4 + \text{C}_2\text{H}_6 + \text{C}_3\text{H}_8 + \text{CO}_2$		
151	5.06	276.7
105	7.0	272.8

Table 3. Langmuir Parameters (Parrish and Prausnitz¹³)

gas	small cavities		large cavities	
	$10^3 A/\text{K}\cdot\text{MPa}^{-1}$	B/K	$10^2 A/\text{K}\cdot\text{MPa}^{-1}$	B/K
Structure I				
CH_4	36.7592	2708.8	18.1363	2737.9
C_2H_6	0	0	6.8174	3631.6
C_3H_8	0	0	0	0
CO_2	11.8243	2860.5	8.3979	3277.9
Structure II				
CH_4	29.1807	2695.1	75.0918	2202.7
C_2H_6	0	0	40.2942	3038.4
C_3H_8	0	0	12.1945	4406.1
CO_2	8.9743	2695.4	47.6426	2571.8

value can be compared with the one measured by Song and Kobayashi⁸ on the same gas mixture and at the same pressure with $x(\text{H}_2\text{O}) = 427 \cdot 10^{-6}$ which is the closest data point with our measurements. The hydrate dissociation temperature was 277.2 K.

The gas mixture 2 was studied at 4.0 MPa with $x(\text{H}_2\text{O})$ equal to $(190 \pm 10) \cdot 10^{-6}$ and $(290 \pm 15) \cdot 10^{-6}$, and the same mixture has been considered at a pressure of 1.3 MPa with $x(\text{H}_2\text{O})$ equal to $(233 \pm 12) \cdot 10^{-6}$. The water content in the vapor phase versus temperature curves were shown in Figure 2. The determined hydrate dissociation temperatures were respectively (274.4, 280.2, and 266.2) K.

The gas mixture 3 was studied at (5.06 and 7.0) MPa with respectively $x(\text{H}_2\text{O})$ equal to $(151 \pm 8) \cdot 10^{-6}$ and $(105 \pm 5) \cdot 10^{-6}$. The determined hydrate dissociation temperatures were respectively (276.7 and 272.8) K (Figure 3).

Table 2 gives a summary of the determined hydrate dissociation temperatures for the three different mixtures.

Modeling Study. As in our previously work, we have used the van der Waals and Platteeuw model¹¹ to model the chemical potential (or fugacity) of water in the hydrate phase and the CPA equation of state for the fluid phase.

The fugacity of water in the hydrate phase is expressed as follows:

$$f_w^H = f_w^{\text{MT}} \exp\left[\frac{-\Delta\mu_w^H}{RT}\right] \quad (1)$$

The fugacity of water in the empty hydrate lattice, f_w^{MT} , is expressed as follows:

$$f_w^{\text{MT}} = P_w^{\text{MT}} \varphi_w^{\text{MT}} \exp\left[\frac{V_w^{\text{MT}}(P - P_w^{\text{MT}})}{RT}\right] \quad (2)$$

where $\exp[(V_w^{\text{MT}}(P - P_w^{\text{MT}}))/(RT)]$ is the Poynting correction, P_w^{MT} the vapor pressure of water in the empty hydrate lattice, φ_w^{MT} the fugacity coefficient of water in the empty hydrate lattice, P the pressure, and V_w^{MT} the molar volume of water in the empty

Table 4. Critical Properties and Acentric Factor

component	T_c/K	P_c/MPa	ω
water	647.37	22.12	0.344
methane	190.6	4.6	0.0110
ethane	305.4	4.88	0.099
propane	369.83	4.25	0.152
carbon dioxide	304.2	7.38	0.2250

Table 5. Comparison between Experimental and Calculated Hydrate Dissociation Temperatures Obtained without an Aqueous Phase

$10^6 x(\text{H}_2\text{O})$	P/MPa	T_{exp}/K	supposed hydrate structures ^a	$T_{\text{model}}/\text{K}$
Gas Mixture 1: $\text{CH}_4 + \text{C}_3\text{H}_8$				
137	5.0	275.0	sII	275.0
391	2.07	279.8	sII	277.1
427 ⁸	2.07	277.2	sII	278.1
Gas Mixture 2: $\text{CH}_4 + \text{C}_2\text{H}_6 + \text{CO}_2$				
190	4.0	274.4	sI	275.5
290	4.0	280.2	sI	280.6
233	1.3	266.2	sII	264.0
Gas Mixture 3: $\text{CH}_4 + \text{C}_2\text{H}_6 + \text{C}_3\text{H}_8 + \text{CO}_2$				
151	5.06	276.7	sII	275.8
105	7.0	272.8	sII	274.6

^a Calculated with Gibbs free analysis on large amounts of water content.

hydrate which is considered to be independent of the pressure. The value of P_w^{MT} is very small, in general between (0.01 and 1) kPa. Therefore, φ_w^{MT} is set equal to unity. The Sloan correlations² are used to calculate P_w^{MT} for structures I and II, respectively:

$$\ln(P_w^{\text{MT}}/\text{Pa}) = 28.953 - \frac{6003.9}{(T/\text{K})} \quad (3)$$

$$\ln(P_w^{\text{MT}}/\text{Pa}) = 28.845 - \frac{6017.6}{(T/\text{K})} \quad (4)$$

The value of V_w^{MT} , used in eq 2, was taken from Parrish and Prausnitz.¹³

The chemical potential difference of water between the empty hydrate lattice and the filled hydrate lattice was given by the van der Waals and Platteeuw model:¹¹

$$\Delta\mu_w^H = -RT \sum_m v_m \ln(1 - \sum_j \theta_{mj}) \quad (5)$$

where θ_{mj} denotes the fractional filling of cavity m by guest molecules j and v_m denotes the cavity number per water molecule in the hydrate structure. According to the Langmuir adsorption theory, θ_{mj} can be obtained by:

$$\theta_{mj} = \frac{C_{mj} f_j}{(1 + \sum_k C_{mk} f_k)} \quad (6)$$

where f_j is the fugacity of the gas species j in the vapor phase and C_{mj} is the Langmuir constant which determines the affinity of gas molecules j to occupy the cavities m . The Parrish and Prausnitz¹³ model was used to calculate C_{mj} :

$$C_{mj}(T) = \frac{A_{mj}}{(T/\text{K})} \exp\left(\frac{B_{mj}}{(T/\text{K})}\right) \quad (7)$$

The A_{mj} and B_{mj} parameters values are given in Table 3. To calculate the fugacity of water in hydrate, we need information about their structures. As we do not have access experimentally to them, we assume that the structures with low water content are the same as those with large amounts of water. The latter

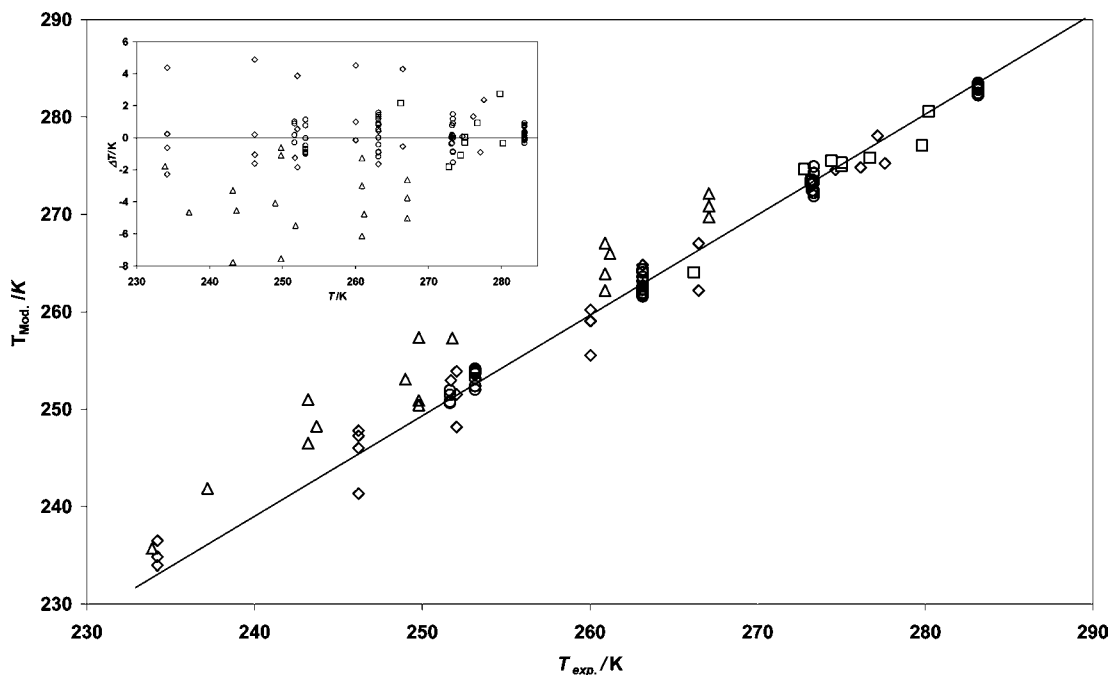


Figure 4. Comparison between experimental and modeling dissociation temperatures of hydrates without the aqueous phase. \square , this work; \triangle , Song and Kobayashi;⁸ \diamond , Aoyagi and Kobayashi;⁹ \circ , Chapoy et al.¹⁰ The insert graph shows the deviation between experimental data and modeling (ΔT) as a function of temperature.

Table 6. Average Deviation between the Different Data Sets and the Modeling Approach

reference	number of data	number of mixtures	average deviation (K)
Aoyagi and Kobayashi ⁹	17	2	4.0
Chapoy et al. ¹⁰	54	2	0.7
Song and Kobayashi ⁸	23	1	1.7
this work	7	3	1.2
overall			1.5

are determined by our model (or others of the open literature) with a stability analysis on Gibbs free energy.¹⁴ These structures are given in Table 5.

The CPA equation of state^{15,16} is used to calculate water and host molecule fugacities in the vapor phase, f_w^V . It has been shown that the CPA equation gave good predictions of the dissociation temperature for methane hydrate, ethane hydrate, and carbon dioxide hydrate.^{12,17} For nonassociating compounds, the CPA equation requires the critical properties and the acentric factor. They are given in Table 4. For associating compounds, the CPA equation requires five parameters: three parameters for the physical part, a_0 , C_1 , and b ; and two for the association part, the association energy ϵ and the association volume β . a_0 and C_1 are two parameters in the energy term. b is the covolume parameter.

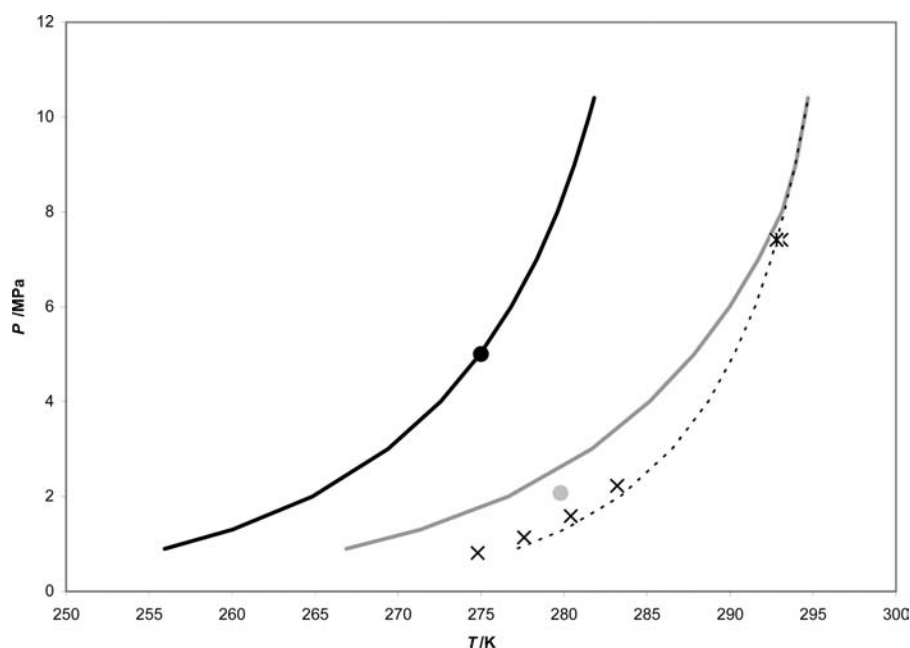


Figure 5. Hydrate–vapor equilibrium curve of gas mixture 1 calculated by using the CPA equation of state. Comparison between experimental data and the CPA equation of state. Vapor–hydrate equilibrium with $x(\text{H}_2\text{O}) = 137 \cdot 10^{-6}$: \bullet , this work; $-$, CPA. Vapor–hydrate equilibrium with $x(\text{H}_2\text{O}) = 391 \cdot 10^{-6}$: \bullet , this work; $-$, CPA. Vapor–liquid aqueous–hydrate equilibrium: \times , Deaton and Frost;¹⁸ $*$, Thakore and Holder;¹⁹ $----$, CPA.

The parameter values for water are given by Kontogeorgis et al.¹⁶ The four-site association scheme (4C) is applied for water. No binary interaction parameter is used in the CPA equation.

The combination of the van der Waals and Platteeuw model for the hydrates and the CPA equation of state for the vapor phase has been used without any fitting adjustment on our new data. All of their parameters have been obtained on other phase equilibria (liquid–vapor for CPA and with large excess of water for the hydrate approach). This approach is then extrapolated to the specific equilibrium of hydrate and vapor with low water content; it is used in a totally predictive way.

Results and Discussion

In Table 5, we compared our experimental hydrate dissociation temperatures without any aqueous phase with the hydrate dissociation temperatures calculated by using the developed approach; we have also included a data point of literature.⁸ Figure 4 shows the comparison diagram of hydrate dissociation temperature between the available data and the model. We can observe that the model is able to estimate the dissociation temperature well for a large range of conditions: from (233 to 280) K and for different gas mixture compositions. The average absolute deviation is about 1.5 K for 105 data points including our measurements. These latest have an absolute deviation about 1.2 K. Table 6 shows the detailed average deviations for each set of data, and the insert graph in Figure 4 shows that there is no specific deviation as a function of temperature: some data are overestimated, and some others are underestimated. The largest deviations are obtained for the lower temperatures and high pressures. We have also compared these data sets with the semiempirical approach detailed in Chapoy et al.,¹⁰ and we have obtained the same results with an average deviation of 2.2 K.

The interest of the associative term of the CPA equation of state to describe the fugacities of the fluid phase should be also evaluated. We have realized the same kind of calculation using the classical Soave–Redlich–Kwong (SRK) equation instead of CPA. As previously, the SRK equation has been used without any binary parameter. We obtain larger deviations; the absolute average deviation is about 17 K. This result shows the useful contribution of the associative term so as to better represent the fluid phase properties.

Another advantage of the CPA equation of state to model the fluid behavior is shown in Figure 5. In this temperature–pressure phase diagram, the hydrate–vapor equilibrium and the hydrate–liquid water curves predicted by the CPA equation of state are plotted and compared with experimental data. The model is able to reproduce our measurements without the aqueous liquid phase. Some experimental data in the presence of the aqueous phase are also reported.^{18,19} In the latter case, the calculation of CPA is equally in agreement with the published data. We can conclude that the classical Platteeuw and van der Waals model associated with the CPA equation of state correctly predicts the hydrate equilibrium with and without the aqueous phase. Finally, it should be noticed that the binary interaction parameters in the CPA equation should be used to improve the results. These binary parameters should be determined on fluid phase equilibrium when the operating range of conditions has been defined.

Conclusion

In this work, the new experimental procedure developed in our previous work was used to determine the hydrate dissociation temperature in the absence of any aqueous phase on three gas mixtures at different pressures and for different water

amounts. As previously, it has been demonstrated that the classical Platteeuw and van der Waals model associated with the CPA equation of state correctly predicts hydrate dissociation with or without the aqueous phase for the gas mixtures. The strength of the associative term of the CPA equation has been also well-illustrated: it is not possible to describe such experimental data using the classical SRK equation of state without binary parameters. It should emphasize that, in this work, the CPA equation of state is used without binary parameters and it is then extrapolated to the specific equilibrium of hydrate and vapor with low water content; it is used in a totally predictive way.

Literature Cited

- (1) Hammerschmidt, E. G. Formation of gas hydrate in natural gas transmission lines. *Ind. Eng. Chem.* **1934**, *26*, 851–855.
- (2) Sloan, E. D. *Clathrate Hydrates of Natural Gases*, 2nd ed.; Marcel Dekker Inc.: New York, 1998.
- (3) Carroll, J. J. *Natural Gas Hydrates: A Guide for Engineers*; Elsevier Science: Amsterdam, 2003.
- (4) Aoyagi, K.; Song, K. Y.; Kobayashi, R.; Sloan, E. D.; Dharmawardhana, P. B. *Water content and correlation of the water content of methane in equilibrium with hydrates II. The water content of a high carbon dioxide simulated Prudhoe Bay gas in equilibrium with hydrates*, Gas Proc. Assn. Res. Report No. 45: Tulsa, OK, December 1980.
- (5) Song, K. Y.; Yarrison, M.; Chapman, W. Experimental low temperature water content in gaseous methane, liquid ethane, and liquid propane in equilibrium with hydrate at cryogenic conditions. *Fluid Phase Equilib.* **2004**, *224*, 271–277.
- (6) Song, K. Y.; Kobayashi, R. The water content of ethane, propane and their mixtures in equilibrium with liquid water or hydrates. *Fluid Phase Equilib.* **1994**, *95*, 281–298.
- (7) Song, K. Y.; Kobayashi, R. Water content of CO₂ in equilibrium with liquid water and/or hydrates. *SPE Form. Eval.* **1987**, 500–508.
- (8) Song, K. Y.; Kobayashi, R. Measurement and interpretation of the water of a methane-propane mixture in the gaseous state in equilibrium with hydrate. *Ind. Eng. Chem. Fundam.* **1982**, *21*, 391–395.
- (9) Aoyagi, K.; Kobayashi, R. *Report of water content measurement of high carbon dioxide content simulated Prudhoe Bay gas in equilibrium with hydrates*, Proc. 57th Annual Convention, Gas Processors Association, New Orleans, LA, March 20–23, 1978; p 3.
- (10) Chapoy, A.; Haghighi, H.; Burgess, R.; Tohidi, B. Gas hydrate in low water content gases: experimental measurements and modelling using the CPA equation of state. *Fluid Phase Equilib.* **2009**; DOI: 10.1016/j.fluid.2009.11.026.
- (11) van der Waals, J. H.; Platteeuw, J. C. Clathrate solutions. *Adv. Chem. Phys.* **1959**, *2*, 2–57.
- (12) Youssef, Z.; Barreau, A.; Mougin, P.; Jose, J.; Mokbel, I. Measurement of hydrate dissociation temperature of methane, ethane and CO₂ in the absence of any aqueous phase and prediction with the Cubic Plus Association equation of state. *Ind. Eng. Chem. Res.* **2009**, *48*, 4045–4050.
- (13) Parrish, W. R.; Prausnitz, J. M. Dissociation pressures of gas hydrates formed by gas mixtures. *Ind. Eng. Chem., Process Des. Dev.* **1972**, *11*, 26–34.
- (14) Ballard, A. L.; Sloan, E. D. The next generation of hydrate prediction: an overview. *J. Supramol. Chem.* **2002**, *2*, 385–392.
- (15) Kontogeorgis, G. M.; Voutsas, E. C.; Yakoumis, I. V.; Tassios, D. P. An equation of state for associating fluids. *Ind. Eng. Chem. Res.* **1996**, *35*, 4310–4318.
- (16) Kontogeorgis, G. M.; Yakoumis, I. V.; Meijer, H.; Hendriks, E. M.; Moorwood, T. Multicomponent phase equilibrium calculations for water-methanol-alkane mixtures. *Fluid Phase Equilib.* **1999**, *158–160*, 201–209.
- (17) Haghighi, H.; Chapoy, A.; Burgess, R.; Mazloun, S.; Tohidi, B. Phase equilibria for petroleum reservoir fluids containing water and aqueous methanol solutions: experimental and modelling using the CPA equation of state. *Fluid Phase Equilib.* **2009**, *278*, 106–116.
- (18) Deaton, W. M.; Frost, E. M. *Gas hydrates and their relation to the operation of natural-gas pipe lines*; U.S. Bureau of Mines Monograph 8, 1964; p 101.
- (19) Thakore, J. L.; Holder, G. D. Solid vapor azeotropes in hydrate-forming systems. *Ind. Eng. Chem. Res.* **1987**, *26*, 462–469.

Received for review November 25, 2009. Accepted May 3, 2010.

JE901001U